

Daala: A Perceptually-Driven Next Generation Video Codec

Thomas J. Daede^{*†}, Nathan E. Egge^{*†}, Jean-Marc Valin^{*†}, Guillaume Martres^{*‡},
Timothy B. Terriberry^{*†}

^{*}Xiph.Org Foundation
21 College Hill Road
Somerville, MA 02144
United States

[†]Mozilla
331 E. Evelyn Ave.
Mountain View, CA 94041
United States
tterribe@xiph.org

[‡]EPFL
Route Cantonale
1015 Lausanne
Switzerland

Copyright 2015-2016 Mozilla Foundation. This work is licensed under [CC-BY 4.0](#).

Abstract

The Daala project is a royalty-free video codec that attempts to compete with the best patent-encumbered codecs. Part of our strategy is to replace core tools of traditional video codecs with alternative approaches, many of them designed to take perceptual aspects into account, rather than optimizing for simple metrics like PSNR. This paper documents some of our experiences with these tools, which ones worked and which did not, and what we've learned from them. The result is a codec which compares favorably with HEVC on still images, and is on a path to do so for video as well.

Introduction

Since its inception, Daala has used lapped transforms [1]. These promise to structurally eliminate blocking artifacts from the transform stage, one of the most annoying artifacts at low bitrates [2, 3]. Although extended to variable block sizes and block sizes up to 16×16 for still images [4], extensions to the larger block sizes found in modern codecs become problematic due to the exponential search complexity. We now use a fixed-lapping scheme that admits an easy search and improves visual quality despite a lower theoretic coding gain.

Daala also employs OBMC [5] to eliminate blocking artifacts from the prediction stage. Early work demonstrated improvements simply by running OBMC as a post-process to simple block-matching algorithms [6]. This was later extended to multiple block sizes, including adaptively determining the overlap [7], but still running as a post-process. We use a novel structure borrowed from surface simplification literature that allows efficient searching and partition size selection using the actual prediction, instead of a block-copy approximation.

Daala also builds on the vector quantization work of the Opus audio codec [8], extending its gain-shape quantization scheme to support predictors and adaptive entropy coding [9]. We explicitly encode the gain of bands of AC coefficients, that is, their contrast, and explicitly code how well each band matches the predictor. By extracting a small number of perceptually meaningful parameters like this from an otherwise undifferentiated set of transform coefficients, this “Perceptual Vector Quantization” enables a host of new techniques. We have demonstrated its use for automatic

activity masking (to preserve detail in low-contrast regions) [9] and frequency-domain Chroma-from-Luma (CfL) to enhance object boundaries in the color planes [10].

Both lapped transforms and PVQ are particularly susceptible to ringing artifacts, the former due to the longer basis functions and the latter due to the tendency either to skip entire diagonal bands (giving artifacts on diagonal edges similar to wavelets) or to inject energy into the wrong place when trying to preserve contrast. Furthermore, lapping prevents strong directional intra prediction, which could be used to create clean edges. Therefore, we designed a sophisticated directional deringing filter, which aggressively filters directional features with minimal side information.

Methodology

This section attempts to describe why we made many of the choices we did. All of the code, including the full commit history, is available in our public git repository [11]. Where appropriate, it includes the four metrics we commonly examine, PSNR, SSIM [12], PSNR-HVS-M [13], and multiscale FastSSIM [14]. Unless otherwise specified, Bjøntegaard-delta [15] (BD) rate changes and other results are from our automated testing framework [16]. By default this uses 18 sequences ranging in resolution from 416×240 to 1920×1080 and 48 to 60 frames in length.

Overall, the codec constructs a frequency-domain predictor for each block, codes the input with PVQ using this predictor, and then filters the result. In intra frames, we construct the predictor with simple horizontal and vertical prediction in the luma plane (copying coefficients) and Chroma-from-Luma in the chroma planes (described below). In inter frames, we construct a motion-compensated reference frame for the whole image using OBMC, and then apply our forward transform to obtain the required frequency-domain predictor. Discussion of the above techniques follows.

Lapped Transforms

Video codecs have used adaptive filters to remove blocking artifacts since the H.263 standard was developed, at least. However, there are also non-adaptive solutions to the blocking problem: lapped transforms. Daala uses the time-domain construction from [3], with the DCT and lapping implemented using reversible lifting transforms.

Originally, we applied lapping in an order similar to that of a loop filter, applying the post-filter to rows of pixels first, for the entire image, and then columns (the pre-filter ran in the opposite order). This allows maximal parallelism with minimal buffering. However, this has two issues. First, it creates strangely-shaped basis functions in the presence of varying block sizes. Although possible to see in synthetic examples, we never observed an issue on real images, and adaptive deblocking filters have a similar issue. Second, it makes block size decisions NP-hard, because you must know the sizes of both the current block and its neighbors in order to determine the amount of lapping to apply, creating a two-dimensional dependency graph that does not admit a tree structure, and thus has no dynamic programming solution.

We developed a heuristic to make up-front block size decisions, without a rate-distortion optimization (RDO) search, based on the estimated visibility of ringing artifacts. However, it made clearly sub-optimal decisions for video, often choosing

large transforms when only a small portion of a block changed. To make a real RDO search tractable, we made two adjustments. First, we made the order recursive: we first apply the lapping to the exterior edges of a 32×32 superblock, then if we are splitting to a 16×16 , we filter the interior edges. This is essentially the same as the order proposed by Dai et al. [4]. Second, we fixed the lapping size to an 8-point filter (4 pixels on either side of a block edge). For 4×4 blocks, we apply 4-point lapping to the interior edges of an 8×8 block (overlapping with the 8-point lapping applied to the exterior edges). When subsampled, the chroma planes always use 4-point lapping.

This removed the dependency on the neighbors' block sizes, allowing for a tree-structured dynamic programming search. This proceeds bottom up. At each level, we start with the optimal block size decision using blocks of at most $N/2 \times N/2$, undo the lapping on the interior edges of the quadtree split, and compare with a single $N \times N$ block. In both cases the exterior edges of the $N \times N$ block remain lapped, but we can at least make an apples-to-apples comparison of the relative distortions.

The result is an optimal solution using blocks of at most $N \times N$. This optimization procedure produced BD-rate reductions of 10.4% for PSNR, and 12.3% for SSIM. On our more perceptual metrics, the changes were smaller: 4.5% for PSNR-HVS-M and 5.2% for multiscale FastSSIM. This reflects the reduction in coding gain from the reduced lapping sizes. These gains are almost entirely due to the improved decisions. Using the same decisions produced by this fixed-lapping process with the previous variable-lapping scheme gave almost as much gain.

Despite the smaller lapping size, this scheme actually increases ringing artifacts. We primarily code edges with 4×4 blocks, but have increased the support of the 4×4 blocks from 8 pixels to 12. To reduce the effects of ringing, we are currently using only 4-point lapping on all block edges. Making this change provided another 3.6% gain in PSNR, and 1.4% on PSNR-HVS-M, but lost 0.4% on multiscale FastSSIM. The visual impact is somewhat larger, and seems to be a regression for intra frames, but a win in some cases on video. This will require more systematic visual testing.

Bilinear Smoothing Filter

Because the smaller lapping size no longer completely eliminates blocking, especially in smooth gradients, we apply a bilinear smoothing filter to all 32×32 blocks in keyframes. The filter simply computes a bilinear interpolation between the four corners of a decoded block (after unlapping). Then, it blends the result of that interpolation with the decoded pixels. Unlike a conventional deblocking filter, it does not look outside of the current block at all.

For a given quantization step size, Q , the optimal Wiener filter gain is

$$w = \min \left(1, \frac{\alpha Q^2}{12D^2} \right), \quad (1)$$

where α is a strength parameter (currently set to 5 for luma and 20 for chroma) and D^2 is the mean squared error between the decoded block and the bilinear interpolation. However, in practice we found that using w^2 works better than w , as it applies less smoothing when we are uncertain if it is a good idea. The result is actually a small

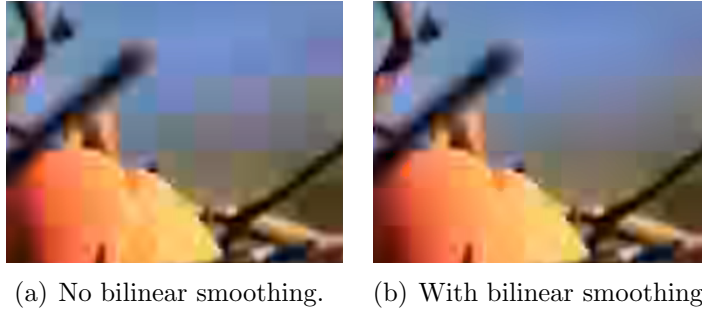


Figure 1: Excerpt from a 1.1 MP image compressed to 4.8 kB (0.035 bpp) (a) without the bilinear smoothing filter and (b) with the bilinear smoothing filter.

(< 1%) regression on metrics on `subset3` [17], our large still image training subset, but provides a substantial visual reduction in blocking in gradients at low rates.

Perceptual Vector Quantization

Perceptual Vector Quantization uses the gain-shape vector quantization found in Opus [8], extended to take advantage of prediction and adaptive entropy coding. The main idea is that it splits the AC coefficients into bands and explicitly codes the magnitude (“gain”), g , of each band. Then, the band is normalized to a unit vector, and the “shape” of the spectrum is encoded separately. To handle prediction, we apply a Householder reflection to map the normalized prediction onto one of the axes, and then code the angle between that axis and the vector being quantized, θ . What remains is a vector on a sphere of dimension $N - 1$ (where N here is the size of the band) with a known radius $g \sin \theta$. We normalize and code this vector using Pyramid Vector Quantization [18] to reduce the number of degrees of freedom to $N - 2$, eliminating any redundancy with g and θ . For details, we refer readers to [9].

One thing this provides is explicit energy preservation, which is less important for video than audio, and can even be relaxed to save bits during RDO. More importantly, the gain directly encodes the contrast in each band. This allows us to implement activity masking without sending any extra side information. Instead of using a linear quantizer, we compand the gain to get more resolution for smaller gains. Then, once we know the gain, we adjust the quantizer used for θ and the shape vector to give more bits to smooth regions where errors are easily visible, and fewer bits to textured regions where they are not. We disable activity masking on 4×4 blocks to avoid over-penalizing edges.

Chroma-from-Luma Prediction

Although color conversion to $Y'C_bC_r$ decorrelates the color channels globally across the frame, there is still some local correlation. Lee and Cho created a spatial domain chroma predictor using a linear model of the relationship between chroma and luma built from previously-decoded neighbors [19]. Because Daala uses lapped transforms, these neighbors are unavailable when they are needed. Although it would be possible,

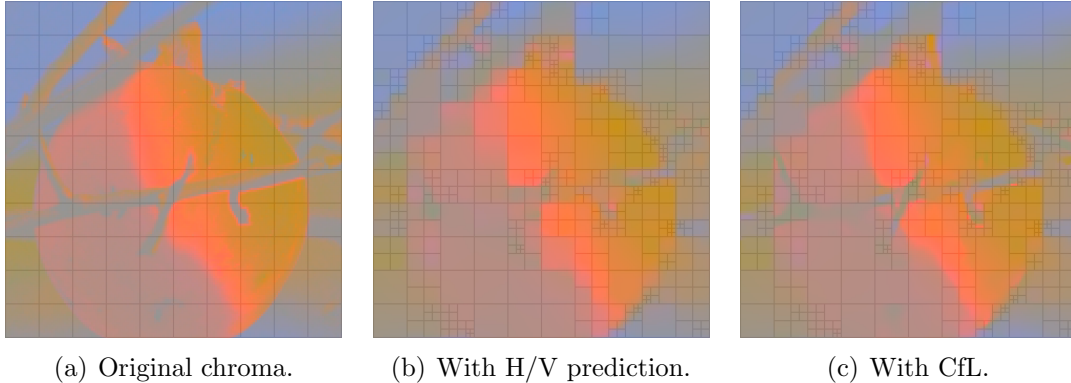


Figure 2: Example comparison of (a) the original chroma planes with (b) horizontal and vertical spatial prediction and (c) Chroma-from-Luma prediction.

with additional complexity, to use more distant neighbors, this technique is even more efficient in the frequency domain. PVQ even makes it possible to remove the model fitting step entirely. For more details, see [10].

We predict the chroma shape in PVQ directly from the luma coefficients. We assume that frequency-domain chroma AC coefficients $C_{AC}(u, v)$ are linearly related to their co-located luma AC coefficients $L_{AC}(u, v)$, and that both have zero mean. This linear model is exactly what is needed to create a chroma *shape* predictor, \mathbf{r} , for a band of AC coefficients from the reconstructed luma coefficients in that band, $\hat{\mathbf{L}}_{AC}$.

$$C_{AC}(u, v) = \alpha_{AC} \cdot L_{AC}(u, v) \implies \mathbf{r} = \alpha_{AC} \cdot \hat{\mathbf{L}}_{AC} \quad (2)$$

While the value of α_{AC} can be learned in the decoder, it is sometimes wrong. It is cheaper to simply code its sign (its magnitude is already represented by PVQ's $g \sin \theta$). This technique allows us to predict features within a block that cannot be predicted by straight edge extension. Although this significantly reduces the number of bits spent on chroma, the perceptual impact is even larger, giving cleaner edges than the horizontal and vertical intra prediction we use for the luma plane.

Deringing Filter

The use of lapped transforms and the lack of directional intra prediction, along with the energy preservation of PVQ [9], make Daala particularly susceptible to ringing artifacts. To combat this, Daala uses an in-loop deringing filter that takes into account the direction of edges and patterns being filtered. On keyframes, this runs before the bilinear smoothing filter. The filter identifies the direction of each block and adaptively filters along that direction. A second filter runs across the lines filtered by the first filter, with more conservative thresholds to avoid blurring edges. We describe the process in some detail here, since it has not been published elsewhere.

First, the decoder splits the image into 8×8 blocks, and determines a dominant direction for each block from the decoded image. These directions do not need to be transmitted, reducing the overhead of side information for the filter. A perfectly

0	0	1	1	2	2	3	3
1	1	2	2	3	3	4	4
2	2	3	3	4	4	5	5
3	3	4	4	5	5	6	6
4	4	5	5	6	6	7	7
5	5	6	6	7	7	8	8
6	6	7	7	8	8	9	9
7	7	8	8	9	9	10	10

(a) Example line partitions.

Index	Direction	d_x	d_y
0	↗	1	-1
1	→	1	$-\frac{1}{2}$
2	→	1	0
3	↘	1	$\frac{1}{2}$
4	↘	1	1
5	↓	$\frac{1}{2}$	1
6	↓	0	1
7	↙	$-\frac{1}{2}$	1

Direction	d_x	d_y
↓	0	1
↓	0	1
↓	0	1
↓	0	1
↓	0	1
→	1	0
→	1	0
→	1	0

(b) Direction parameters.

(c) Second stage.

Figure 3: Line numbers for pixels following one direction in an 8×8 block and the steps between pixels for each direction for each filter stage. Pixels are always sampled using nearest-neighbor filtering, with no subpel filter.

directional block would have a constant value along all lines in a given direction. The decoder minimizes the “mean squared difference” (MSD) between the decoded block and a perfectly directional block formed by taking the mean of the pixels in each line.

For each direction, d , we partition the pixels into distinct lines, as illustrated in Fig. 3(a), indexing the lines by k . The MSD, σ_d^2 , is then

$$\sigma_d^2 = \frac{1}{N} \sum_{k=0}^{N_d-1} \left[\sum_{p \in P_{d,k}} (x_p - \mu_{d,k})^2 \right], \quad (3)$$

where $P_{d,k}$ is the set of pixels in line k following direction d , x_p is the value of the pixel at location p , N_d is the number of lines in the block with direction d , and N is the size of the block. $\mu_{d,k}$ is the pixel average for the k^{th} line in direction d :

$$\mu_{d,k} = \frac{1}{N_{d,k}} \sum_{p \in P_{d,k}} x_p, \quad (4)$$

where $N_{d,k}$ is the number of pixels in $P_{d,k}$.

Substituting (4) into (3) and simplifying, we get

$$\sigma_d^2 = \frac{1}{N} \left[\sum_{p \in \text{block}} x_p^2 - \sum_{k=0}^{N_d-1} \frac{1}{N_{d,k}} \left(\sum_{p \in P_{d,k}} x_p \right)^2 \right]. \quad (5)$$

The first term is constant. The optimal direction, d_{opt} , is then just

$$d_{\text{opt}} = \max_d s_d, \quad (6)$$

where

$$s_d = \sum_{k=0}^{N_d-1} \frac{1}{N_{d,k}} \left(\sum_{p \in P_{d,k}} x_p \right)^2 . \quad (7)$$

The decoder still selects a direction for blocks with no strong directional features. The goal is to allow stronger filtering without crossing directional edges.

We use a “conditional replacement filter” to remove noise without blurring sharp edges, like a median or bilateral filter, but simpler and easier to vectorize with SIMD:

$$y(n) = x(n) + \frac{1}{W} \sum_{k=-M}^{k=M} w_k \text{thresh}(x(n+k) - x(n), T) , \quad (8)$$

with the threshold function

$$\text{thresh}(d, T) = \begin{cases} d, & |d| < T , \\ 0, & \text{otherwise.} \end{cases} \quad (9)$$

The result is a filter where the pixels whose difference from the center pixel, $x(n)$, exceed the threshold T are simply replaced by the value of $x(n)$. This keeps the normalization weight, W , constant, and setting it to a power of two avoids the division.

The first, or “directional” filter is the 7-tap conditional replacement filter

$$y(i, j) = x(i, j) + \frac{1}{W} \sum_{k=1}^3 w_k \left[\text{thresh}(x(i, j) - x(i + [kd_y], j + [kd_x]), T_d) \right. \\ \left. + \text{thresh}(x(i, j) - x(i - [kd_y], j - [kd_x]), T_d) \right] \quad (10)$$

where (i, j) is the pixel location, d_x and d_y are defined in Table 3(b) and T_d is the threshold for the directional filter stage. Since the direction is constant over 8×8 blocks, all operations in this filter are directly vectorizable.

We choose the weights w_k to be $\mathbf{w} = [3 \ 2 \ 2]$ with $W = 16$. Although ringing is *roughly* proportional to the quantization step size, Q , as the quantizer increases the error grows less than linearly because the unquantized coefficients become very small compared to Q . We start with a power model of the form

$$T_0 = \alpha_1 Q^\beta , \quad (11)$$

with $\beta = 0.842$ and $\alpha_1 = 1$, which were chosen by manually testing thresholds for $Q = 5$ and $Q = 400$ (on a linear scale). We can use a stronger filter on more directional blocks, both because they have more ringing, and because there is less chance of blurring non-directional features. Blocks that are less directional require a weaker filter. We estimate the degree of directionality, δ , as the difference between the optimal variance and the variance along the orthogonal direction:

$$\delta = |\sigma_{d_{\text{opt}}}^2 - \sigma_{(d_{\text{opt}}+4) \bmod 8}^2| = s_{d_{\text{opt}}} - s_{(d_{\text{opt}}+4) \bmod 8} . \quad (12)$$

The final threshold is then

$$T_d = T_0 \cdot \max \left(\frac{1}{2}, \min (3, \alpha_2 (\delta \cdot \delta_{\text{sb}})^{0.16}) \right), \quad (13)$$

where δ_{sb} is the average of δ over a 32×32 superblock and $\alpha_2 = 1.02$.

The second filter stage is always horizontal or vertical, and operates across the directional lines used in the first filter:

$$z(i, j) = y(i, j) + \frac{1}{W} \sum_{k=1}^2 w_k \left[\text{thresh} (y(i, j) - y(i + [kd_y], j + [kd_x]), T_d) \right. \\ \left. + \text{thresh} (y(i, j) - y(i - [kd_y], j - [kd_x]), T_2(i, j)) \right] \quad (14)$$

where d_x and d_y are defined in Table 3(c) and $T_2(i, j)$ is a position-dependent threshold for the second stage. Since the second filter risks blurring edges, and its input has less ringing than the first, it only has 5 taps and a conservatively chosen $T_2(i, j)$:

$$T_2(i, j) = \min \left(T_d, \frac{T_d}{3} + |y(i, j) - x(i, j)| \right). \quad (15)$$

We choose the filter weights to be $\mathbf{w} = [3 \ 3]$ with $W = 16$.

If a superblock was skipped and is not in an intra frame, it is never deringed. Otherwise, a flag enables or disables deringing for a superblock. Even when enabled, we do not dering 8×8 blocks that were skipped and whose surrounding 4×4 neighbors were also skipped (taken into account because of lapping). The deringing process may read pixels that lie outside the current superblock. When they lie another superblock, we use unfiltered pixel values—even for the second stage filter—to avoid adding a dependency between superblocks. This allows filtering all superblocks in parallel. When they lie outside the image, the threshold function, $\text{thresh}(d, T)$, returns 0.

Subjective Results

Daala participated in the 2015 Picture Coding Symposium evaluation of existing and future still image codecs [20]. This included both objective evaluation with different metrics than those we used during development and subjective evaluation with test subjects drawn from a pool of multimedia quality experts. Daala was compared with five other state of the art codecs including BPG [21] and VP9 [22]. Figure 4 shows the subjective results for two of the six still images tested.

Our best results were on **woman**, a close up portrait of a woman wearing a knit shirt. About two thirds of this image are hair and skin, which contain texture that is well coded using PVQ even at very low rates. Activity masking hides quantization errors in the hair where other codecs end up removing detail by zeroing high frequencies.

The image where Daala had the worst result was **bike**, a picture of a tennis racket leaned against a bike wheel. This picture contains strong directional edges which are well predicted by directional intra prediction. Because Daala only contains a limited set of horizontal and vertical intra predictors, it spends more bits coding regions that are well predicted in other codecs. The version of Daala tested by the competition was also using an earlier prototype of the deringing filter that was less effective.

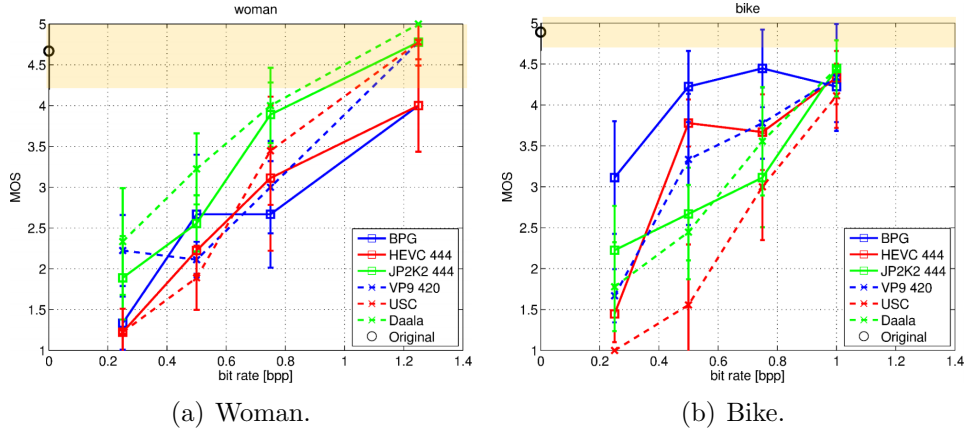


Figure 4: Subjective still-image comparisons of Daala and several competing codec implementations. Shown here are results from the images that gave the (a) best and (b) worst results for Daala.

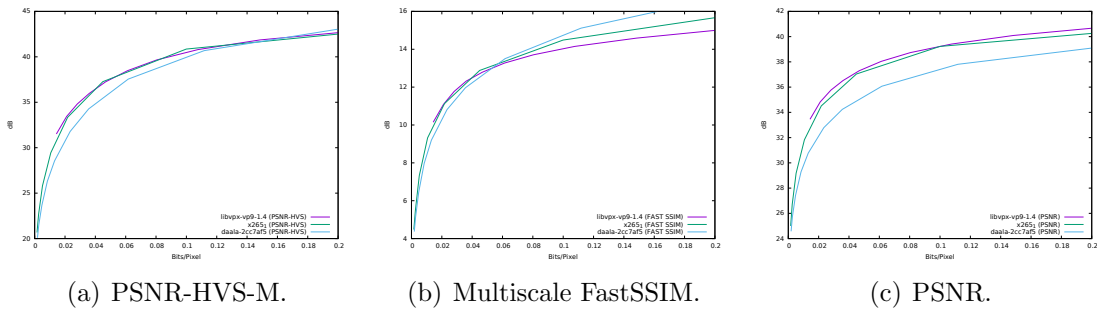


Figure 5: Metric comparisons between Daala, libvpx-vp9 1.4.0, and x265 1.6.

Objective Results

We computed objective results using standard metrics, using implementations in the Daala repository. Daala is compared against x265 1.6 and libvpx-vp9 1.4.0. The comparisons are made automatically by our open-source AreWeCompressedYet tool [16]. Two perceptual metrics are used, PSNR-HVS-M and multiscale FastSSIM [13, 14], as well as PSNR. Daala does much better than the other two codecs at high bit-rates, though there is still room for improvement at lower rates. Daala performs especially well on the perceptual metrics compared to PSNR, as expected when using perceptually-based coding methods. As of this writing, we do not code out-of-order frames (B-frames or alt-refs), so we see substantial room for improvement on video.

References

- [1] N. E. Egge, “Time domain lapped transforms for video coding,” <https://tools.ietf.org/html/draft-egge-netvc-tdlt>, 2012.

- [2] H. S. Malvar and D. H. Staelin, "The LOT: Transform coding without blocking effects," *IEEE Transactions on Acoustics, Speech, and Signal Processing*, vol. 37, no. 4, pp. 553–559, Apr. 1989.
- [3] T. D. Tran, "Lapped transform via time-domain pre- and post-filtering," *IEEE Transactions on Signal Processing*, vol. 51, no. 6, pp. 1556–1571, May 2001.
- [4] W. Dai, L. Liu, and T. D. Tran, "Adaptive block-based image coding with pre-/post-filtering," in *Proceedings of the 2005 Data Compression Conference (DCC'05)*, Salt Lake City, UT, Mar. 2005, pp. 73–82.
- [5] T. B. Terriberry, "Adaptive motion compensation without blocking artifacts," in *Proceedings of Visual Information Processing and Communication VI*, A. Said, O. G. Guleryuz, and R. L. Stevenson, Eds., vol. 9410, San Francisco, CA, Mar. 2015.
- [6] H. Watanabe and S. Singhal, "Windowed motion compensation," in *Proceedings of SPIE Visual Communications and Image Processing '91*, vol. 1605, Nov. 1991, pp. 582–589.
- [7] J. Zhang, M. O. Ahmad, and M. N. S. Swamy, "New windowing techniques for variable-size block motion compensation," *IEE Proceedings—Vision, Image, and Signal Processing*, vol. 145, no. 6, pp. 399–407, Dec. 1998.
- [8] J.-M. Valin, K. Vos, and T. B. Terriberry, "RFC 6716: Definition of the Opus audio codec," <https://tools.ietf.org/html/rfc6716>, 2012.
- [9] J.-M. Valin and T. B. Terriberry, "Perceptual vector quantization for video coding," in *Proceedings of Visual Information Processing and Communication VI*, vol. 9410, San Francisco, CA, Mar. 2015.
- [10] N. E. Egge and J.-M. Valin, "Predicting chroma from luma with frequency domain intra prediction," in *Proceedings of Visual Information Processing and Communication VI*, vol. 9410, San Francisco, CA, Mar. 2015.
- [11] "Daala git repository," <https://git.xiph.org/daala.git>.
- [12] Z. Wang, A. C. Bovik, H. R. Sheikh, and E. P. Simoncelli, "Image quality assessment: From error visibility to structural similarity," *IEEE Transactions on Image Processing*, vol. 13, no. 4, pp. 600–612, Apr. 2004.
- [13] N. Ponomarenko, F. Silvestri, K. Egiazarian, M. Carli, J. Astola, and V. Lukin, "On between-coefficient contrast masking of DCT basis functions," in *CD-ROM Proceedings of the 3rd International Workshop on Video Processing and Quality Metrics for Consumer Electronics (VPQM '07)*, Scottsdale, Arizona, Jan. 2007.
- [14] M.-J. Chen and A. C. Bovik, "Fast structural similarity index algorithm," *Journal of Real-Time Image Processing*, vol. 6, no. 4, pp. 281–287, Dec. 2011.
- [15] T. Daede, "Video codec testing and quality measurement," <https://tools.ietf.org/html/draft-daede-netvc-testing>, 2015.
- [16] "Are we compressed yet?" <https://arewecompressedyet.com/>.
- [17] "Daala test media," https://wiki.xiph.org/Daala.Quickstart#Test_Media.
- [18] T. R. Fischer, "A pyramid vector quantizer," *IEEE Transactions on Information Theory*, vol. 32, no. 4, pp. 568–583, Jul. 1986.
- [19] S.-H. Lee and N.-I. Cho, "Intra prediction method based on the linear relationship between the channels for YUV 4:2:0 intra coding," in *Image Processing (ICIP), 2009 16th IEEE International Conference on*, Nov. 2009, pp. 1037–1040.
- [20] "Picture Coding Symposium 2015 feature event: Evaluation of current and future image compression technologies," <http://www.pcs2015.org/>.
- [21] "Better portable graphics (BPG)," <http://bellard.org/bpg/>.
- [22] "VP9 video codec," <https://www.webmproject.org/vp9/>.